Interdisciplinary Information Sciences Vol. 29, No. 2 (2023) 157–168
©Graduate School of Information Sciences, Tohoku University
ISSN 1340-9050 print/1347-6157 online
DOI 10.4036/iis.2023.R.02

A Mathematical Consideration on the Relation of the Social Structure to the Infection Risk in a Community

Elza Firdiani SOFIA* and Hiromi SENO

Department of Computer and Mathematical Sciences, Graduate School of Information Sciences, Tohoku University, Sendai 980-8579, Japan

We construct and analyze a mathematical model to consider the relation of the social structure to the infection risk for a spreading transmissible disease in a community. We take into account different phases of human activity, whether it takes place solely in the private situation or both private and social spheres, followed by the division of the community members into two classes: active and less active. The analysis on our mathematical model implies that there are critical conditions for the class size and human activity with respect to the infection risk for a community. Further, we try to discuss how the social structure and situation could be related to the infection risk for a community.

KEYWORDS: epidemics, mathematical model, infection risk, social structure, human activity

1. Introduction

In recent times, the global spread of COVID-19 has been a constant fight for many communities [9], especially with the high human-to-human transmissibility via respiratory droplets and airborne particles containing the virus [4]. Human mobility is one of the relevant factors that could cause the spread of such transmissible diseases. As phones are usually carried by the users in the recent decades, their cellular activities and locations may be regarded as indices to represent the level of user's activities and mobility in such a way that phones may be considered as a platform for sensing human activity distributed in a large scale [6]. It was demonstrated that such a mobility data derived from phone can be utilized to draw a correlation between the social distancing and the growth of COVID-19 infection within USA [2, 17, 30, 31]. In Japanese major metropolitan areas, Nagata *et al.* [20] found that a decrease of mobility, especially in nightlife-related districts, preceeded a reduction in COVID-19 incidences. In UK, utilizing a smartphone data and location geotagging collected by social media, Jeffrey *et al.* [16] found that British people reduced their social activity following the order of social distancing. In Taiwan, Chang *et al.* [5] used a metapopulation models with a social media location data in order to identify areas with a high risk of disease spread. These previous works imply that a rise of activity is followed by an increase of new cases, and to some extent, a fall in activity results in a decrease of new cases. Yabe *et al.* [33] and Zhang *et al.* [34] report and summarize the studies regarding the correlation between human mobility and COVID-19 transmission according to the data usage, modeling, and key findings.

In the pandemic of COVID-19, many researches have been piled up to understand the nature of disease spread from a variety of scientific viewpoints not only on the influence of human mobility but also on the other demographic factors. Some of them observe the actual dependence of the spread on the social structure in the community which is represented by the age distribution, the household composition, the economic disparities, the coresidence pattern etc. (for example [3, 8, 10, 13, 18, 19, 21]). Such factors must be essentially related to the epidemic dynamics through a contribution to the contact with the pathogen which causes the spread of a transmissible disease. In a most general sense, a higher social activity could be regarded as the social situation to induce a larger likeliness to contact with the pathogen. The activity level must depend on the social factors related to its kinetics and organization, which has been observed in the researches mentioned before.

In this work, we shall take the viewpoint to consider the relation of social structure on the infection risk in a community, and construct and analyze a mathematical model to discuss it. In our modeling, the infection risk is indexed by the expected number of new cases. We take into account the activity level and the sphere where the activity takes place, according to the type of social interaction held. With the mathematical results obtained by the analysis on our model, we shall try to discuss the relation of the social activity level and sphere to the infection risk for a community. Differently from most of theoretical works to concern the prevalence or epidemic size in a community with a given social situation/structure, we shall focus on the social structure of a community itself according to how easy or fast a

Received October 19, 2022; Accepted February 20, 2023; J-STAGE Advance published April 21, 2023
HS was supported in part by JSPS KAKENHI Grant Number 18K03407 and 22K03430. We thank the editor and two anonymous reviewers for their valuable comments and suggestions to finalize the manuscript.
*Corresponding author. E-mail: elzsafir@gmail.com

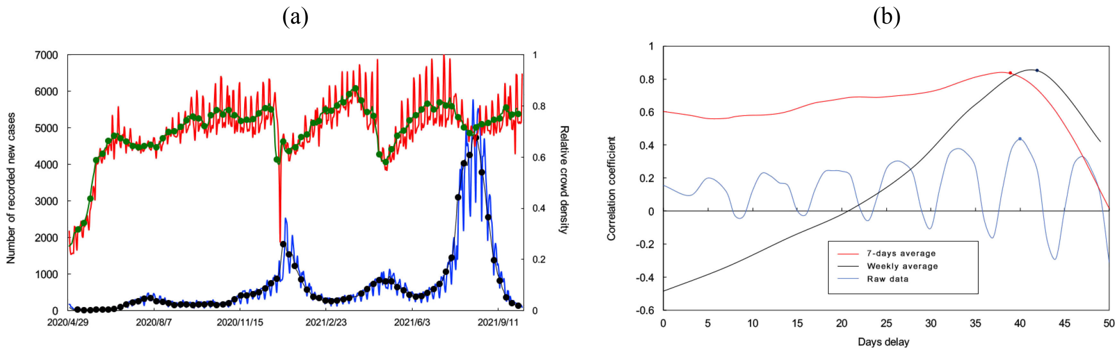

Fig. 1. (a) Plots of a data on the relative crowd density in Shibuya crossing by the MSS and recorded new COVID-19 cases in Tokyo Metropolitan area from May 2020 to September 2021 [14, 23]. The upper plots in (a) indicate the relative crowd density where the weekly average is drawn together. (b) The dependence of the correlation coefficient on the days delay about the raising crowd density and increasing number of new cases. The lower fluctuating graph in (b) indicates the number of new cases. The weekly average is drawn together in (a) and (b). The detail about the derivation of (b) from the data of (a) is given in Appendix A.

transmissible disease spreads, for the purpose to theoretically discuss how the difference in the social structure could cause a difference in the epidemic result.

2. Correlation of Human Activity and New Cases

Figure 1(a) shows a data of social activity and new cases, which original data is created by the NTT DOCOMO mobile spatial statistics (MSS) that estimates the population from the operation data of the mobile phone network in Japan as described by Terada *et al.* [27]. Hara and Yamaguchi [11] used the MSS to find a trend in travel during and after the early wave of COVID-19. Their results showed that there were a significant reduction in trips and a decrease in population density index by 20% nationwide as people avoided traveling to crowded areas. Arimura *et al.* [1] reported a reduction in travel as much as 70–80% in the same way. Tsuboi *et al.* [28] gave the corresponding result by their statistical analysis on the MSS with respect to the relation of people's mobility to the number of new cases. Further similar results are found in [22, 24, 26].

Here we focus on the area of Shibuya crossing, one of the most crowded spots in Tokyo, Japan. We have the population distribution dataset provided by the Cabinet Secretariat of the Government of Japan [23] and the daily recorded new cases reported by the Japan Broadcasting Cooperation [14]. The crowd density concluded from the population distribution dataset could be regarded as reflecting the human activity in the local Tokyo community. By our calculation described in Appendix A to derive a reasonable correlation coefficient between human activity and the number of new cases, we found that there must be a positive correlation between them [see Fig. 1(b)], in agreement with the result obtained by the previous works [28, 30, 33] to imply that increased mobility positively contributes to the spread of COVID-19. There must be a lag between the temporal change and peaks in the new cases and those in the crowd density because the reported new cases are accompanied with the latent period and the period for the detection after the infection. As shown in Fig. 1(b), our calculation on the data results in about 40 days lag that could give the greatest correlation coefficient between them. Although this lag seems much longer than the averaged latent period given by the epidemiological research, two weeks for the COVID-19, we could conclude that a certain positive correlation is exemplified between human activity and the new infection, while we could not give any reasonable explanation about such a long time lag.

As demonstrated by our data analysis in this section, it is reasonable to assume that the higher human activity induces the larger number of new cases. Since the human activity level is not determined only by the mobility but also by the other social factors in each social sphere as mentioned in Introduction, we are going to assume a social structure of a community with respect to the activity level, and subsequently construct and analyze a mathematical model in the following sections.

3. Mathematical Modeling of the Infection Risk for a Community

We assume a community which is composed with two classes based on their activity level in daily life: less-active and active. The *less-active class* typically includes elderly and infant who do not spend a significant portion of their day outside their residential area. The *active class* members partake their activities both in the residential area and public places out of it (Fig. 2).

Let us assume here only two different phases about the activity sphere as previously done by Seno [25]: private and social phases. *Private phase* is defined as the activity sphere mainly in the residential area with limited interactions, for

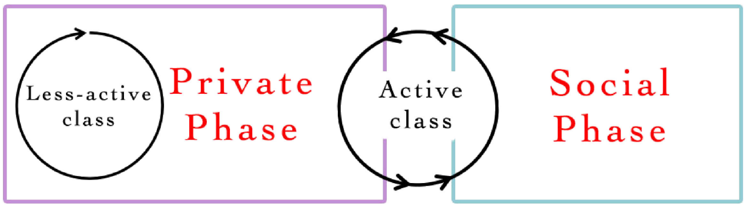

Fig. 2. The activity class and sphere in our modeling.

example, with the family members, neighbors, and house staff. Traveling by personal car or bicycle is considered to be at the private phase. At the *social phase*, the interactions are with arbitrary members of the community in the public sphere which may include work, school, shops, public transportation, etc. The less-active class members have activities only at the private phase, while the active class members have those at both the private and social phases.

At the private phase, infectious contact between members of two classes is possible. In contrast, infectious contact at the social phase happens only between members of the active class. The likelihood of infection is assumed to be different according to the interaction that takes place at each phase, contributed by both the active and less-active classes at the private phase and solely by the active class at the social phase. The member of less-active class has a likelihood to get infected only at the private phase. The member of active class has a likelihood to get infected at the private or social phase. Higher risk of infection must result in a higher expected number of new cases.

Expected number of new cases for the less-active class

Let N denote the population size of the community. The sizes of active and less-active classes are given by qN and $(1-q)N$, respectively with the ratio of active class q in the community. Now we define the expected number of new cases in an appropriate time unit for the less-active class as

$$E_l(\alpha, q) = \beta_p(\alpha, q)(1-q)N, \tag{3.1}$$

where $\beta_p = \beta_p(\alpha, q)$ is the probability of infection for an individual per unit time at the private phase. We introduce here a constant parameter α $(0 < \alpha < 1)$ that indexes the mean proportion of time at the social phase in a daily life for the member of active class. Since β_p depends on the class size and activity level of both active and less-active members, E_l is denoted here as a function of α and q in general. To proceed with the analytical investigation on our mathematical model, we will give a specific function for $\beta_p = \beta_p(\alpha, q)$ later.

Expected number of new cases for the active class

Let $\alpha\beta_s$ be the probability for an individual of active class to get infected at the social phase, and $(1-\alpha)\beta_p$ be the probability at the private phase. β_s corresponds to the probability of infection for an individual per unit time at the social phase. Then, the individual of active class can avoid getting infected at the private and social phases and being uninfected with probability $\{1-(1-\alpha)\beta_p\}(1-\alpha\beta_s)$. Hence, the infection occurs for the individual of active class with probability $1-\{1-(1-\alpha)\beta_p\}(1-\alpha\beta_s)$. The probability β_s depends on α and q as well as β_p: $\beta_s = \beta_s(\alpha, q)$. Therefore, we define the expected number of new cases for the active class as

$$E_a(\alpha, q) = [1 - \{1-(1-\alpha)\beta_p(\alpha, q)\}\{1-\alpha\beta_s(\alpha, q)\}]qN. \tag{3.2}$$

Infection risk for the community

The infection risk for the community is now represented by the expected number of new cases defined by $E(\alpha, q) = E_l(\alpha, q) + E_a(\alpha, q)$ where $E_l(\alpha, q)$ and $E_a(\alpha, q)$ are given by (3.1) and (3.2). In this paper, we introduce the following formulas for probabilities β_s and β_p:

$$\beta_s = \beta_s(\alpha, q) = \sigma_s\alpha qN; \quad \beta_p = \beta_p(\alpha, q) = \sigma_p\{(1-q)N + (1-\alpha)qN\}, \tag{3.3}$$

where αqN corresponds to the expected population density at the social phase, and $(1-q)N + (1-\alpha)qN$ does to that at the private phase. Positive constants σ_s and σ_p are the infection coefficients at the social and private phases, respectively. This formulation is based on the assumption that the infection probability has a positive correlation to the population density in accordance with the arguments in Sect. 2. For the well definition of probabilities β_s and β_p, our modeling with (3.3) leads to a confinement of parameters σ_s and σ_p such that $\sigma_s N \leq 1$ and $\sigma_p N \leq 1$.

In the following sections, we will consider the dependence of E to parameters q and α. These parameters characterize the community structure and situation. Parameter q may correspond to the characteristic hardly changeable (age structure, for example) in the epidemic dynamics, while α may be changeable like the behavioral nature of the active class in the community, which could be influenced by governmental policy, social perception, campaign, education, and so on. Focusing on these two parameters, we will try to discuss how the infection risk depends on the social structure.

4. Dependence of the Infection Risk on the Class Size

We can get the following result about the q-dependence of the expected number of new cases E (Appendix B):

Theorem 4.1. *The expected number of new cases E is monotonically decreasing in terms of* $q \in (0, 1)$ *if and only if* $\alpha \le \alpha_c$*, where* α_c *is given by the unique root of the cubic equation*

$$-3\alpha^3 + 5\alpha^2 + 2A\alpha - \frac{2}{\sigma_s N} = 0 \tag{4.1}$$

for $\alpha \in (0, 1)$ *with*

$$A := \frac{1}{\sigma_s N} + \frac{1}{\sigma_p N} - 1. \tag{4.2}$$

Otherwise when $\alpha > \alpha_c$*, E has a unique extremal minimum at* $q = q^* \in (0, 1)$ *where*

$$q^* = \begin{cases} \dfrac{1}{3(1-\alpha)\alpha}\left\{-(A+\alpha) + \sqrt{(A+\alpha)^2 + \dfrac{6(1-\alpha)}{\sigma_s N}}\right\} & \text{for } \alpha \in (\alpha_c, 1); \\ \dfrac{1/(\sigma_s N)}{1/(\sigma_s N) + 1/(\sigma_p N)} & \text{for } \alpha = 1. \end{cases} \tag{4.3}$$

When the active class has the social phase sufficiently longer than the private phase, there is a certain proportion of active class for which the expected number of new cases becomes minimum. Otherwise, the expected number of new cases is smaller as the size of active class gets larger.

5. Dependence of the Infection Risk on the Activity

We can get the following result on the α-dependence of the expected number of new cases E (Appendix C):

Theorem 5.1. *The expected number of new cases E is monotonically decreasing in terms of* $\alpha \in (0, 1)$ *if and only if*

$$q \le q_c := \frac{3}{2} + A - \sqrt{\left(\frac{3}{2} + A\right)^2 - \frac{2}{\sigma_s N}}, \tag{5.1}$$

where A is given by (4.2). Otherwise when $q > q_c$*, E has a unique extremal minimum at* $\alpha = \alpha^*$ *which is the unique root of*

$$-4\alpha^3 + 3\left(1 + \frac{1}{q}\right)\alpha^2 + \frac{2A}{q}\alpha - \frac{2}{\sigma_s N q^2} = 0 \tag{5.2}$$

for $\alpha \in (0, 1)$.

When the active class is sufficiently larger than the less-active class, there is a certain proportion of the social phase for which the expected number of new cases becomes minimum. Otherwise, the expected number of new cases becomes smaller as the proportion of the social phase gets larger.

6. Social Structure to Minimize the Infection Risk

First we find the following result from the theorems obtained in the previous section:

Corollary 6.1. *The expected number of new cases E cannot become minimum for* $\alpha = 0$ *or* $q = 0$.

The case of $\alpha = 0$ is the situation in which the members of active class always stay at the private phase, in other words, every individual in the community is of the less-active class. Such a situation could be regarded as the community under the complete lockdown. Hence, this result implies that the complete lockdown could not minimize the infection risk in the community. Therefore, the expected number of new cases E may become minimum when (α, q) is one of the following cases: $(1, 1)$; $(1, q^*)$; $(\alpha^*, 1)$ with $\alpha^* \in (0, 1)$ and $q^* \in (0, 1)$.

The case of $(\alpha, q) = (1, 1)$ could be taken into account only when $\alpha \le \alpha_c \in (0, 1)$ and $q \le q_c \in (0, 1)$ because this is the case when E is monotonically decreasing in terms of $\alpha \in (0, 1)$ and $q \in (0, 1)$ as shown in the previous theorems. Thus, the case when $\alpha = 1$ and $q = 1$ is contradictory to the condition. Therefore, the case of $(\alpha, q) = (1, 1)$ cannot make E minimum. The case of $(\alpha, q) = (1, 1)$ is corresponding to the situation such that every individual belongs to the active class and always has activities at the social phase. This result matches our intuition that the highest active situation would be worse with respect to the infection risk. We can prove in the same way that the case of $(1, q^*)$ cannot make E minimum, and further that the case of (α^*, q^*) cannot exist.

Consequently we have the following result (Appendix D):

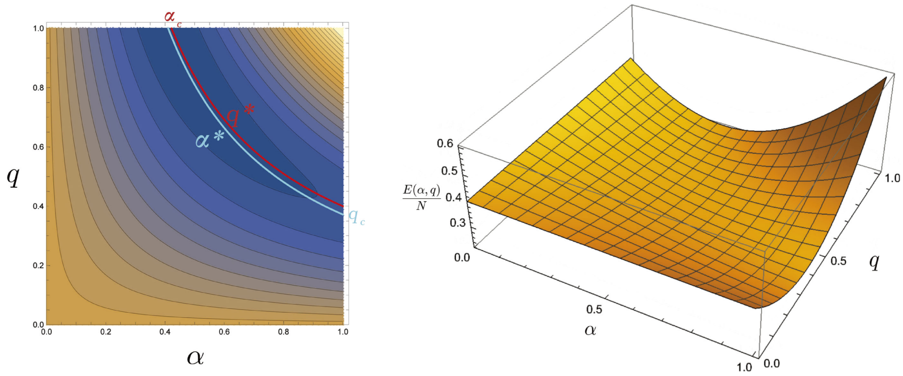

Fig. 3. Numerically obtained (α, q)-dependence of $E(\alpha, q)$ with $\sigma_s N = 0.6$, $\sigma_p N = 0.4$, $q_c = 0.372$, and $\alpha_c = 0.42152$. Contour map (left) and 3-dimensional graph (right).

Theorem 6.1. *The expected number of new cases E becomes minimum for* $(\alpha, q) = (\alpha^*, 1)$ *such that* $0 < \alpha^* \leq \alpha_c < 1$.

This result is visualized by the numerical calculation in Fig. 3. It is theoretically implied that the situation with no less-active class minimizes the infection risk, whereas such a situation in an established community could not be realistic in general. On the other hand, a specific situation in a temporarily organized village like that in the Olympiad may be applicable. Then, Theorem 6.1 implies that the infection risk could be minimized by controlling the daily schedule in the village to an appropriate extent about the activity there.

As for the dependence of $E(\alpha^*, 1)$ on parameters $\sigma_s N$ and $\sigma_p N$, we find that $E(\alpha^*, 1)/N$ becomes larger as $\sigma_s N$ or $\sigma_p N$ gets larger. This is an intuitively expected result because the larger $\sigma_s N$ or $\sigma_p N$ means the higher risk at the social or private phase.

7. Restriction for the Management of Infection Risk

From the results about the q-dependence and α-dependence of E obtained in the previous sections, we find that the management of infection risk is significantly restricted by the social structure, and get the following result:

Corollary 7.1. *The expected number of new cases E becomes minimum for* $\alpha = 1$ *when* $q \leq q_c$*, while it becomes minimum for* $q = 1$ *when* $\alpha \leq \alpha_c$.

The situation of $\alpha = 1$ means that the active class is always at the social phase. That is, the members of active class are never at the private phase. This may be regarded as a complete separation of the active class from the less-active one, or of the less-active class from the active one. However, it cannot be adapted for the community-level risk management about the spread of a transmissible disease because such a complete separation of active and less-active classes can be hardly realized. In general, the proportion of active class q is hardly changed as mentioned in Sect. 3. On the other hand, it would be possible to control the proportion of the social phase α. For example, limiting the office work, the school time, or prohibiting from going out for a certain period may be imposed to manage the infection risk. Hence, the above results imply a perspective for the community-level management of infection risk to control the activity of active class, even though there must be a restriction for the changeable range of activity (i.e., α).

As every community is characterized by its own α and q, we could classify communities according to the restriction on the management of infection risk, following our results obtained above. Now, we categorize the social structure into three types as shown in Fig. 4: Type I community for $q \leq q_c$, Type II for $q > q_c$ and $\alpha \leq \alpha_c$, Type III for $q > q_c$ and $\alpha > \alpha_c$.

Let us think of three different communities: one located in an urban metropolis with high mobility and relatively young population, one located in a semi-urban city with a relatively young population but limited options of activity, and another one in a rural area with low mobility and an aging population. In a situation without pandemics, we can imagine that the urban and semi-urban communities have larger size of active class compared to their rural counterparts. The active class in the urban population may have a significantly more options of public settings to spend their proportion of activity sphere in daily life, i.e., at the social phase. Meanwhile, the semi-urban community limits their time spent at the social phase as the activities of its active class are limited only to school/work in different locations and going home afterwards. The rural community will be content to spend their time at the private phase, socializing among neighbors and only a handful of chances to have a huge event where all members of the community come together. It is obvious that the urban community belongs to the Type III, semi-urban one belongs to the Type II, while the rural community one may fall into Type I community.

For Type I community, the expected number of new cases becomes smaller as the proportion of the social phase gets

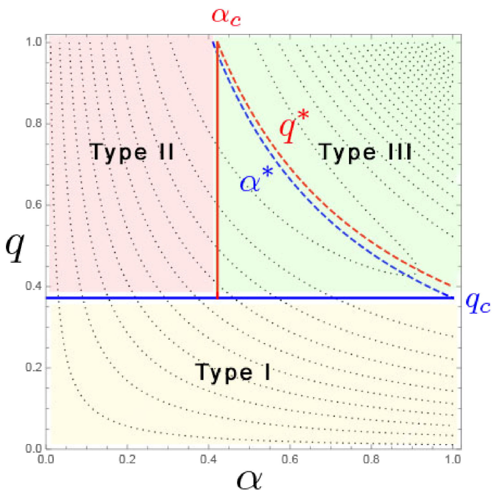

Fig. 4. Classification of the social structure indexed by (α, q). Numerically drawn with parameter values, same with those for Fig. 3.

larger. Therefore, the reduction of time at the social phase could not be appropriate to reduce the infection risk in such a community, which could be regarded as a modern aged community with a large proportion of aged people.

Type II community has a relatively large active class with a sufficiently small proportion of the social phase. Such a community would be characterized by a specific custom of social activities including working, which provides a daily life with a sufficiently short time for the social activity. For example, the case is a community with sufficiently effective telecommunication and teleworking which do not necessarily require the direct contact with the others for a long duration in the daily life. Then, many people could be regarded as being at the private phase for relatively longer duration in the daily life. Our analysis implies that, the same as Type I, the longer time spent at the social phase makes the smaller number of new cases in such a community of Type II. Therefore, for Type II community, in order to reduce the infection risk, it would be effective to promote the social activity out of the private phase. If such a promotion is rather successful, the community of Type II may change to Type III with the longer time spent at the social phase.

Differently from those of Type I and II, the community of Type III has a specific proportion of the social phase to minimize the infection risk as seen in Fig. 4. Hence, for such a community, an appropriate control of the duration at the social phase would be successful to make the infection risk lower.

In the event of pandemic, we can turn our attention back to the urban community of Type III, where there may be a need to control the duration at the social phase into a specific one tailored to reduce the infection risk. Applying policies such as closing shopping center and restaurants early to limit activities, teleworking, online classes and so on, may be appropriate in this type of community to shorten their length of social phase. Periodic closure of public facilities may have a special effect in minimizing a disease spread [12]. However, we need to recall that there must be a possibility of infection at the private phase. With the active class members crowding inside their residential area, the infection may spread still, even worse, putting elderly or infant members of less-active class. For the semi-urban community of Type II, it is much easier to control the spread as they have already a limited duration at the social phase voluntarily due to lifestyle. However, similar to infection spread within homes in the Type I communities, promoting activities at the social phase may be necessary to manage the infection risk.

8. Community with a High Consciousness of the Prevention

In a community with a high consciousness of the prevention against the spread of a transmissible disease, we may assume that the probability of infection could be sufficiently small at both of private and social phases, even when it must depend on the community structure and situation.

For such a community, our modeling follows sufficiently small values of $\sigma_s N$ and $\sigma_p N$ in (3.3). Then, for $\sigma_s N \ll 1$ and $\sigma_p N \ll 1$, we can easily find that

$$\alpha_c \approx \frac{1/(\sigma_s N)}{1/(\sigma_s N) + 1/(\sigma_p N)}; \quad q_c \approx \frac{1/(\sigma_s N)}{1/(\sigma_s N) + 1/(\sigma_p N)} \tag{8.1}$$

from (4.1) in Theorem 4.1 and (C.1) in Appendix C for Theorem 5.1. This result indicates that the classification of community type discussed in the last section can be adopted independently of how little serious a transmissible disease spreading in a community.

The result (8.1) indicates that the classification of community significantly depends on the relative likelihood of infection at each activity sphere. If the probabilities of infection at private and social phases have only a slight difference, the result (8.1) leads to $\alpha_c \approx 0.5$ and $q_c \approx 0.5$. Then our arguments in the last section would be still acceptable because each of three types of community: Type I, II, and III, are defined for a considerable range of social structure represented by parameters α and q in our modeling.

Since those parameters $\sigma_s N$ and $\sigma_p N$ express the infection risk at social and private phases respectively, and they must be strongly correlated with each other, these arguments imply that the discussion in the last section would be applicable to consider a daily policy for the public health, even when the infection risk for a transmissible disease is low.

9. Concluding Remarks

Disease spread is influenced by people's willingness to adopt preventative public health behaviors, which are often associated with public risk perception. Risk perception is correlated significantly with the adoption of preventative health behaviors in ten countries as previously studied [7]. Even for the same disease, the response of communities in a country is dependent on the distinctive institutional arrangements and cultural orientation, affecting the community behavior as a whole [32]. For example, facing COVID-19, governments of the world employ different policies such as "nudge" in Sweden, "mandate" in China, "decree" in France, and "boost" in Japan, with different levels of enforcement and types of strategy [32]. Further, as mentioned in Introduction, the result of such governmental policy and community response about the epidemics must depend on the social structure in the community [3, 8, 10, 13, 18, 19, 21].

We made a suggestive calculation to give the values in Table 1 from the real data on the population size and working statistics for 2020 about some countries. As a value corresponding to our q, we calculated $\hat{q}$ as the ratio of the working age population over 15–64 years old to the total population. For those countries shown in the table, it results in around 0.6–0.7. The calculated value $\hat{\alpha}$ is a reference which might correspond to our α, whereas $\hat{\alpha}$ is calculated from the data of average annual hours actually worked per person in employment, and it would be shorter than our α, because α reflects the time at the social phase which contains some non-working time too. If we apply the values $(\hat{\alpha}, \hat{q})$ in Table 1 for our result, those countries in the table are all Type II defined in Sect. 7. However, the unit of country would be too large to be considered in the framework of our mathematical model. The community structure with respect to the activity related to the infection risk must be heterogeneous in such a large scale of population. In this sense, our work presented here could be regarded as concerning an appropriately small scale of population which could be characterized by the structure with respect to such an activity.

It must be remarked that our modeling follows an assumption that the members of active and less-active classes have interaction between them, so that the assumed community must be defined as a regional community for a daily life. Further we need a statistical or theoretical way to estimate the values of $\sigma_s N$ and $\sigma_p N$ in order to get the values corresponding to q_c and α_c. These values are regarded as the supremum for the infection probability at the social and private phases respectively, and hence they could be regarded as important indices in epidemiological sense. Thus it would be valuable to consider such a statistical or theoretical way to estimate the supremum for the infection probability at a specified sphere of human activity. It is beyond the scope of our research in this paper, and we expect that such related researches could serve the further development of the theoretical and perspective consideration of the socio-epidemiological dynamics on the epidemics of a transmissible disease.

In this work, we considered a mathematical model about the infection risk for a community which consists of two classes based on its activity: active and less-active. The active class has activities in the public and private spheres while the less-active class has the activities only in the private sphere. Every community has its own proportion of

Table 1. Demographic data and tentatively calculated values $\hat{q}$ and $\hat{\alpha}$. Total population (thousands) $\hat{N}$ from World Population Prospects 2022 by United Nations [29], working age population over 15–64 years old (ten thousands) $\hat{W}$, and average annual hours actually worked per person in employment $\hat{H}$ from Databook of International Labour Statistics 2022 by Japan Institute for Labour Policy and Training [15]. $\hat{q}$ denotes $\hat{W}/\hat{N}$, and $\hat{\alpha}$ is calculated as $\hat{H}/(365 \times 5/7)/24$. Values $\hat{N}$, $\hat{W}$, and $\hat{H}$ are all for 2020.

country	$\hat{N}$	$\hat{W}$	$\hat{H}$	$\hat{q}$	$\hat{\alpha}$
Japan	125,543	7,482	1,598	0.596	0.26
USA	335,388	21,514	1,767	0.641	0.28
Canada	37,758	2,496	1,644	0.661	0.26
UK	66,951	4,322	1,367	0.646	0.22
Germany	83,268	5,392	1,332	0.648	0.21
France	64,458	4,020	1,402	0.624	0.22
Italy	59,640	3,852	1,559	0.646	0.25
Sweden	10,321	627	1,424	0.607	0.23
Rep. Korea	51,858	3,674	1,908	0.708	0.30
Australia	25,544	1,645	1,683	0.644	0.27

active and less-active classes, and its active class can be characterized by its behavior at the activity phase. It is clear that there is a dependence of the infection risk for the community upon the community structure and activity. Sufficiently large active class requires a certain duration at the social phase to minimize the infection risk. Longer duration at the social phase reduces the infection risk for a community with sufficiently small active class. When the active class has a sufficiently long social phase, there is a certain size of active class to minimize the infection risk. The active class size and the duration at the social phase can be used to classify the community into different types with particular characteristics that could be utilized to build a better strategy to reduce the infection risk.

As a whole, from those results by the analysis on the model, the complete lockdown such that everyone is forced to be at the private phase would not be an optimal strategy in managing the infection risk. This conclusion may be different from our intuitive thought, because the mobility of active people could be regarded as a relevant factor to increase the contacts between individuals so as to increase the likelihood of secondary infection. However, since there must exist a certain infection risk at the private phase, the complete lockdown results in the higher density at the private phase, that is, the closer contact between individuals at the private phase. Therefore, there is a certain trade-off relation between the risks at two phases, that should be taken into account for making a better policy to manage the infection risk for a community.

Although our work is theoretical and based on a simple mathematical model, the model gave us an insight into the characterization of community and how, in light of disease spread, an efficient control measure that suits the community character could be formulated to manage the infection risk. Further exploration of the infection coefficients and inclusion of more factors into the model, such as visitors from outside the community, control measure by vaccination, and so on may be meaningful to characterize the communities and steps that can be taken to manage the spread of infectious diseases.

REFERENCES

[1] Arimura, M., Ha, T., Okumura, K., and Asada, T., "Changes in urban mobility in Sapporo city, Japan due to the Covid-19 emergency declarations," *Transportation Research Interdisciplinary Perspective*, **7**: 100212 (2020).

[2] Badr, H., Du, H., Marshall, M., Dong, E., Squire, M., and Gardner, L., "Association between mobility patterns and COVID-19 transmission in the USA: A mathematical modelling study," *Lancet Infectious Diseases*, **20(11)**: 1247–1254 (2020).

[3] Banik, A., Nag, T., Chowdhury, S. R., and Chatterjee, R., "Why do COVID-19 fatality rates differ across countries? An explorative cross-country study based on select indicators," *Global Business Review*, **21(3)**: 607–625 (2020).

[4] Centers for Disease Control and Prevention (CDC), *Scientific Brief: SARS-CoV-2 Transmission*. https://www.cdc.gov/coronavirus/2019-ncov/science/science-briefs/sars-cov-2-transmission.html. Retrieved June 15th 2022.

[5] Chang, M., Kahn, R., Li, Y., Lee, C., Buckee, C., and Chang, H., "Variation in human mobility and its impact on the risk of future COVID-19 outbreaks in Taiwan," *BMC Public Health*, **21(1)**: 1–10 (2021).

[6] Doyle, J., Hung, P., Farrell, R., and McLoone, S., "Population mobility dynamics estimated from mobile telephony data," *Journal of Urban Technology*, **21(2)**: 109–132 (2014).

[7] Dryhurst, S., Schneider, C., Kerr, J., Freeman, A., Recchia, G., van Der Bles, A., Spiegelhalter, D., and van Der Linden, S., "Risk perceptions of COVID-19 around the world," *Journal of Risk Research*, **23(7–8)**: 994–1006 (2020).

[8] Dudel, C., Riffe, T., Acosta, E., van Raalte, A., Strozza, C., and Myrskylä, M., "Monitoring trends and differences in COVID-19 case-fatality rates using decomposition methods: Contributions of age structure and age-specific fatality," *PLoS ONE*, **15(9)**: e0238904 (2020).

[9] Du Toit, A., "Outbreak of a novel coronavirus," *Nature Reviews Microbiology*, **18(3)**: 123–123 (2020).

[10] Esteve, A., Permanyer, I., Boertien, D., and Vaupel, J. W., "National age and coresidence patterns shape COVID-19 vulnerability," *Proceedings of the National Academy of Sciences*, **117(28)**: 16118–16120 (2020).

[11] Hara, Y., and Yamaguchi, H., "Japanese travel behavior trends and change under COVID-19 state-of-emergency declaration: Nationwide observation by mobile phone location data," *Transportation Research Interdisciplinary Perspectives*, **9**: 100288 (2021).

[12] Hindes, J., Bianco, S., and Schwartz, I., "Optimal periodic closure for minimizing risk in emerging disease outbreaks," *PLoS One*, **16(1)**: e0244706 (2021).

[13] Hou, X., Gao, S., Li, Q., Kang, Y., Chen, N., Chen, K., Rao, J., Ellenberg, J. S., and Patz, J. A., "Intracounty modeling of COVID-19 infection with human mobility: Assessing spatial heterogeneity with business traffic, age, and race," *Proceeding of the National Academy of Sciences*, **118(24)**: e2020524118 (2021).

[14] Japan Broadcasting Cooperation (Nippon Housou Kyoku; NHK), *Special site for COVID-19*. https://www3.nhk.or.jp/news/special/coronavirus/data/. Retrieved October 3rd 2021.

[15] Japan Institute for Labour Policy and Training, *Databook of International Labour Statistics*. https://www.jil.go.jp/kokunai/statistics/databook/ Retrieved October 1st 2022.

[16] Jeffrey, B., Walters, C., Ainslie, K., Eales, O., Ciavarella, C., Bhatia, S., Hayes, S., Baguelin, M., Boonyasiri, A., Brazeau, N., Cuomo-Dannenburg, G., Fitzjohn, R. G., Gaythorpe, K., Green, W., Imai, N., Mellan, T. A., Mishra, S., Nouvellet, P., Unwin, H. J. T., Verity, R., Vollmer, M., Whittaker, C., Ferguson, N. M., Donnelly, C. A., and Riley, S., "Anonymised and aggregated crowd level mobility data from mobile phones suggests that initial compliance with COVID-19 social distancing interventions was high and geographically consistent across the UK," *Wellcome Open Research*, **5(170)**: 170 (2020).

[17] Jiao, J., Bhat, M., and Azimian, A., "Measuring travel behavior in Houston, Texas with mobility data during the 2020 COVID-19 outbreak," *Transportation Letters*, **13(5–6)**: 461–472 (2021).

[18] Kashnitsky, I., and Aburto, J. M., "COVID-19 in unequally ageing European regions," *World Development*, **136**: 105170

(2020).
[19] Medford, A., and Trias-Llimós, S., "Population age structure only partially explains the large number of COVID-19 deaths at the oldest ages," *Demographic Research*, **43**: 533–544 (2020).
[20] Nagata, S., Nakaya, T., Adachi, Y., Inamori, T., Nakamura, K., Arima, D., and Nishiura, H., "Mobility change and COVID-19 in Japan: Mobile data analysis of locations of infection," *Journal of Epidemiology*, **31(6)**: 387–391 (2021).
[21] Nepomuceno, M. R., Acosta, E., Alburez-Gutierrez, D., Aburto, J. M., Gagnon, A., and Turra, C. M., "Besides population age structure, health and other demographic factors can contribute to understanding the COVID-19 burden," *Proceedings of the National Academy of Sciences*, **117(25)**: 13881–13883 (2020).
[22] Nouvellet, P., Bhatia, S., Cori, A., Ainslie, K., Baguelin, M., Bhatt, S., Boonyasiri, A., Brazeau, N., Cattarino, L., Cooper, L. V., Coupland, H., Cucunuba, Z. M., Cuomo-Dannenburg, G., Dighe, A., Djaafara, B. A., Dorigatti, I., Eales, O. D., van Elsland, S. L., Nascimento, F. F., Fitzjohn, R. G., Gaythorpe, K. A. M., Geidelberg, L., Green, W. D., Hamlet, A., Hauck, K., Hinsley, W., Imai, N., Jeffrey, B., Knock, E., Laydon, D. J., Lees, J. A., Mangal, T., Mellan, T. A., Nedjati-Gillani, G., Parag, K. V., Pons-Salort, M., Ragonnet-Cronin, M., Riley, S., Unwin, H. J. T., Verity, R., Volmer, M. A. C., Volz, E., Walker, P. G. T., Walters, C. E., Wang, H., Watson, O. J., Whittaker, C., Whittles, L. K., Xi, X., Ferguson, N. M., and Donnelly, C. A., "Reduction in mobility and COVID-19 transmission," *Nature Communications*, **121**: 1090 (2021).
[23] Office for COVID-19 and Other Emerging Infectious Disease Control, Cabinet Secretariat, Government of Japan, *Countermeasures against COVID-19 infections: various data*. https://corona.go.jp/dashboard/, Retrieved October 3rd 2021 (in Japanese).
[24] Parady, G., Taniguchi, A., and Takami, K., "Travel behavior changes during the COVID-19 pandemic in Japan: Analyzing the effects of risk perception and social influence on going-out self-restriction," *Transportation Research Interdisciplinary Perspective*, **7**: 100181 (2020).
[25] Seno, H., "An SIS model for the epidemic dynamics with two phases of the human day-to-day activity," *Journal of Mathematical Biology*, **80(7)**: 2109–2140 (2020).
[26] Suppasri, A., Kitamura, M., Tsukuda, H., Boret, S., Pescaroli, G., Onoda, Y., Imamura, F., Alexander, D., Leelawat, N, and Syamsidik, "Perceptions of the COVID-19 pandemic in Japan with respect to cultural, information, disaster and social issues," *Progress in Disaster Science*, **10**: 100158 (2021).
[27] Terada, M., Nagata, T., and Kobayashi, M., "Population estimation technology for mobile spatial statistics," *NTT DOCOMO Technical Journal*, **14(3)**: 10–15 (2013).
[28] Tsuboi, K., Fujiwara, N., and Itoh, R., "Influence of trip distance and population density on intra-city mobility patterns in Tokyo during COVID-19 pandemic," *PLoS ONE*, **17(10)**: e0276741 (2022).
[29] United Nations (UN), Department of Economic and Social Affairs, Population Division, *World Population Prospects 2022, Online Edition*. http://creativecommons.org/licenses/by/3.0/igo/ Retrieved October 1st 2022 (2022).
[30] Xiong, C., Hu, S., Yang, M., Luo, W., and Zhang, L., "Mobile device data reveal the dynamics in a positive relationship between human mobility and COVID-19 infections," *Proceedings of the National Academy of Sciences*, **117(44)**: 27087–27089 (2020).
[31] Xiong, C., Hu, S., Yang, M., Younes, H., Luo, W., Ghader, S., and Zhang, L., "Mobile device location data reveal human mobility response to state-level stay-at-home orders during the COVID-19 pandemic in the USA," *Journal of the Royal Society Interface*, **17(173)**: 20200344 (2020).
[32] Yan, B., Zhang, X., Wu, L., Zhu, H., and Chen, B., "Why do countries respond differently to COVID-19? A comparative study of Sweden, China, France, and Japan," *The American Review of Public Administration*, **50(6–7)**: 762–769 (2020).
[33] Yabe, T., Tsubouchi, K., Fujiwara, N., Wada, T., Sekimoto, Y., and Ukkusuri, S. V., "Non-compulsory measures sufficiently reduced human mobility in Tokyo during the COVID-19 epidemic," *Scientific Reports*, **10(1)**: 1–9 (2020).
[34] Zhang, M., Wang, S., Hu, T., Fu, X., Wang, X., Hu, Y., Halloran, B., Li, Z., Cui, Y., Liu, H., Li, Z., and Bao, S., "Human mobility and COVID-19 transmission: A systematic review and future directions," *Annals of GIS*, **28(4)**: 501–514 (2022).

Appendix A: Steps of Data Analysis

We utilize a population estimation dataset created by the NTT DOCOMO mobile spatial statistics (MSS) which estimates population density using the operation data from mobile phone network. The data estimated hourly population in grids on the basis of phone signal [23]. The recorded densities at 15:00 are used as a reference. We use the relative density at the Shibuya crossing, one of the most crowded spot in Tokyo, Japan as a representative. The daily recorded new case in Tokyo Metropolitan area is taken from the reported cases by the Japan Broadcasting Cooperation [14]. In our calculation on the data, we focus on the datasets from May 2020–October 2021. We adopt the following steps to estimate an appropriate correlation coefficient:

(1) Transformation of the daily data of phone signal into the relative crowd density by normalizing the daily density with the most crowded day between May 2020 to October 2021. It provides the original relative density data. The data of new infection cases is not modified for the original dataset.
(2) For the original relative crowd density and the new infection cases, we obtain the weekly average and seven-days average datasets as well. The weekly average is counted by averaging Monday to Sunday data, while seven-days average is counted as an average from the past seven days including the calculated day (for example, a Wednesday data was obtained by averaging the data from Thursday of its previous week until the Wednesday in question). By now we have the original (raw), weekly average, and seven-days average data for both phone signal and daily case record for crowd density and new cases.

(3) From the datasets, we sample periods between December 2020–January 2021, March–April 2021, and June–July 2021.

(4) The periods with increasing new cases are matched with the crowd density data of the corresponding periods, shifted from zero (recorded cases on the same day) to sixty days.

(5) The correlation coefficients between the reported new cases and crowd density for shifted days are calculated, using the Pearson's correlation coefficient

$$r = \frac{\sum_{i=1}^{n}(x_i - \bar{x})(y_i - \bar{y})}{\sqrt{\sum_{i=1}^{n}(x_i - \bar{x})^2}\sqrt{\sum_{i=1}^{n}(y_i - \bar{y})^2}}.$$

(6) We estimate the number of shifted days to make the correlation coefficient highest as the optimal day(s) delay. The analysis for optimal delay resulted in 40 days for original data ($r = 0.43$), 6 weeks (= 42 days) for weekly average ($r = 0.85$), and 38 days for seven-days average ($r = 0.84$), as indicated in Fig. 1(b).

Appendix B: Proof of Theorem 4.1

From (3.1), (3.2), and (3.3), we have

$$\begin{aligned} E_l(\alpha, q) &= \sigma_p N(1 - \alpha q)(1 - q)N = N \cdot \sigma_p N\{1 - (1 + \alpha)q + \alpha q^2\}; \\ E_a(\alpha, q) &= N \cdot \sigma_p N \sigma_s N\left[(1 - \alpha)\alpha^3 q^2 + \left\{-\frac{1}{\sigma_s N}(1 - \alpha)\alpha + \frac{1}{\sigma_p N}\alpha^2 - (1 - \alpha)\alpha^2\right\}q + \frac{1}{\sigma_s N}(1 - \alpha)\right]q \end{aligned} \tag{B.1}$$

Let us consider

$$\psi(\alpha, q) := \frac{E(\alpha, q)/N}{\sigma_p N \sigma_s N} = (1 - \alpha)\alpha^3 q^3 + (A + \alpha)\alpha^2 q^2 - \frac{2}{\sigma_s N}\alpha q + \frac{1}{\sigma_s N}, \tag{B.2}$$

where A is defined by (4.2), and satisfies that

$$A > \max\left[\frac{1}{\sigma_s N}, \frac{1}{\sigma_p N}\right] > 1,$$

since $\sigma_s N < 1$ and $\sigma_p N < 1$ from the confinement for our modeling. In order to investigate the q-dependence of E, we differentiate (B.2) in terms of q:

$$\begin{aligned} \psi_q(\alpha, q) &:= \frac{\partial \psi(\alpha, q)}{\partial q} = \alpha\left\{3(1 - \alpha)\alpha^2 q^2 + 2(A + \alpha)\alpha q - \frac{2}{\sigma_s N}\right\}; \\ \psi_{qq}(\alpha, q) &:= \frac{\partial^2 \psi(\alpha, q)}{\partial q^2} = \alpha\{6(1 - \alpha)\alpha^2 q + 2(A + \alpha)\alpha\}. \end{aligned} \tag{B.3}$$

Since $\psi_{qq} > 0$ for any $\alpha \in (0, 1)$, ψ_q is monotonically increasing in terms of $q \in (0, 1)$. Since $\psi_q(\alpha, 0) = -2\alpha/(\sigma_s N) \le 0$, there are two distinct cases depending on the sign of $\psi_q(\alpha, 1)$. If $\psi_q(\alpha, 1) \le 0$, then $\psi_q(\alpha, q) < 0$ for $q \in (0, 1)$ so that ψ is monotonically decreasing for any $q \in (0, 1)$, while, if $\psi_q(\alpha, 1) > 0$, then $\psi_q(\alpha, q)$ changes its sign from negative to positive as q gets larger in $(0, 1)$ so that ψ has a unique extremal minimum at a value of $q = q^* \in (0, 1)$. In such a case, the value q^* is the root of the equation $\psi_q(\alpha, q)/\alpha = 0$ in terms of q as given by (4.3), where q^* depends on α.

Further, we can find that

$$\frac{\partial}{\partial \alpha}\left\{\frac{\psi_q(\alpha, 1)}{\alpha}\right\} = 3(2 - 3\alpha)\alpha + 2(A + 2\alpha) = 9\alpha(1 - \alpha) + \alpha + 2A > 0$$

for $\alpha \in (0, 1)$, and

$$\left.\frac{\psi_q(\alpha, 1)}{\alpha}\right|_{\alpha=0} = -\frac{2}{\sigma_s N} < 0; \quad \left.\frac{\psi_q(\alpha, 1)}{\alpha}\right|_{\alpha=1} = 2(A + 1) - \frac{2}{\sigma_s N} = \frac{2}{\sigma_p N} > 0.$$

Thus, there is a unique value $\alpha_c \in (0, 1)$ such that $\psi_q(\alpha, 1) < 0$ for $\alpha < \alpha_c$ and $\psi_q(\alpha, 1) > 0$ for $\alpha > \alpha_c$. We can easily find that the critical value α_c is given by the unique root of the cubic equation (4.1) in terms of $\alpha \in (0, 1)$. These results conclude Theorem 4.1.

Appendix C: Proof of Theorem 5.1

We have the following partial derivatives of $\psi(\alpha, q)$ defined by (B.2) in terms of α:

$$\psi_\alpha(\alpha, q) := \frac{\partial\psi(\alpha, q)}{\partial\alpha} = q^3\left\{-4\alpha^3 + 3\left(1 + \frac{1}{q}\right)\alpha^2 + \frac{2A}{q}\alpha - \frac{2}{\sigma_s N q^2}\right\};$$
$$\psi_{\alpha\alpha}(\alpha, q) := \frac{\partial^2\psi(\alpha, q)}{\partial\alpha^2} = 2q^3\left\{-6\alpha^2 + 3\left(1 + \frac{1}{q}\right)\alpha + \frac{A}{q}\right\}. \tag{C.1}$$

Since $\psi_{\alpha\alpha}(0, q) = 2q^2A > 0$ and $\psi_{\alpha\alpha}(1, q) = 2q^3\{-3 + (3 + A)/q\} > 0$, we can easily find that $\psi_{\alpha\alpha}(\alpha, q) > 0$ for $\alpha \in (0, 1)$. Hence, ψ_α is monotonically increasing for $\alpha \in (0, 1)$.

From (C.1), we have $\psi_\alpha(0, q) = -2q/(\sigma_s N) < 0$ and

$$\frac{\psi_\alpha(1, q)}{q} = -q^2 + (3 + 2A)q - \frac{2}{\sigma_s N}, \tag{C.2}$$

and then,

$$\left.\frac{\psi_\alpha(1, q)}{q}\right|_{q=0} = -\frac{2}{\sigma_s N} < 0; \quad \left.\frac{\psi_\alpha(1, q)}{q}\right|_{q=1} = 2\left(1 + A - \frac{1}{\sigma_s N}\right) = \frac{2}{\sigma_p N} > 0. \tag{C.3}$$

From (C.2) and (C.3), we can easily find that $\psi_\alpha(1, q)$ is negative for $q < q_c \in (0, 1)$ and positive for $q > q_c$, where q_c is given by (5.1) as the smaller root of the equation $\psi_\alpha(1, q)/q = 0$.

Consequently, since ψ_α is monotonically increasing for $\alpha \in (0, 1)$, we have $\psi_\alpha(\alpha, q) \le 0$ for any $\alpha \in (0, 1)$ if and only if $q \le q_c$, while $\psi_\alpha(\alpha, q)$ changes the sign from negative to positive as α gets larger if and only if $q > q_c$. Therefore, $\psi(\alpha, q)$ is monotonically decreasing in terms of $\alpha \in (0, 1)$ if and only if $q > q_c$.

Appendix D: Proof of Theorem 6.1

First, we prove the following lemma:

Lemma D.1. *The expected number of new cases E cannot be minimum for* $(\alpha, q) = (1, q^*)$ *for any* $q^* \in (0, q_c]$.

The case of $(\alpha, q) = (1, q^*)$ could be valid only when $\alpha > \alpha_c \in (0, 1)$ and $q \le q_c \in (0, 1)$ from Theorems 4.1 and 5.1. Thus, it is necessary that $q^* \le q_c$, otherwise this case is invalid for minimizing E. From the proof of Theorem 5.1 in Appendix C, the condition that $q^* \le q_c$ is equivalent to that $\psi_\alpha(1, q^*) \le 0$, that is, from (C.2),

$$-q^{*2} + (3 + 2A)q^* - \frac{2}{\sigma_s N} \le 0.$$

Since q^* is given by (4.3) for $\alpha = 1$, this condition becomes

$$-\left\{\frac{1/(\sigma_s N)}{1/(\sigma_s N) + 1/(\sigma_p N)}\right\}^2 + \left(\frac{2}{\sigma_s N} + \frac{2}{\sigma_p N} + 1\right)\frac{1/(\sigma_s N)}{1/(\sigma_s N) + 1/(\sigma_p N)} - \frac{2}{\sigma_s N} \le 0.$$

With some calculations about this inequality, we can find the equivalent inequality such that $1/(\sigma_p N) \le 0$. This is impossible. Hence the condition $q^* \le q_c$ cannot be satisfied when $\alpha = 1$. Therefore, it has been shown that $q^*|_{\alpha=1} > q_c$. Therefore, the case of $(\alpha, q) = (1, q^*)$ cannot be valid for minimizing E. As a result, we can get Lemma D.1.

Next, the case of $(\alpha, q) = (\alpha^*, 1)$ could be valid for minimizing E only when $\alpha \le \alpha_c \in (0, 1)$ and $q > q_c \in (0, 1)$ from Theorems 4.1 and 5.1. Thus, it is necessary that $\alpha^* \le \alpha_c$ for $q = 1$, otherwise this case is invalid for minimizing E. From Theorem 4.1, the condition that $\alpha^* \le \alpha_c$ is equivalent to that

$$-3\alpha^{*3} + 5\alpha^{*2} + 2A\alpha^* - \frac{2}{\sigma_s N} \le 0. \tag{D.1}$$

Then, from (5.2) in Theorem 5.1, we have α^* for $q = 1$ which satisfies the following equation:

$$-4\alpha^{*3} + 6\alpha^{*2} + 2A\,\alpha^* - \frac{2}{\sigma_s N} = \left(-3\alpha^{*3} + 5\alpha^{*2} + 2A\,\alpha^* - \frac{2}{\sigma_s N}\right) - (\alpha^{*3} - \alpha^{*2}) = 0. \tag{D.2}$$

Hence, from (D.1), we can get the condition that $\alpha^{*3} - \alpha^{*2} = \alpha^{*2}(\alpha^* - 1) \le 0$. This condition is necessarily satisfied if there exists $\alpha^* \in (0, 1)$ when $q = 1$. Indeed, from (D.2), it can be easily seen that there exists uniquely $\alpha^* \in (0, 1)$ even when $q = 1$. From these arguments, we have proved that it is necessarily satisfied that $\alpha^* \le \alpha_c$ when $q = 1$. As a result, we can get the following lemma:

Lemma D.2. *The expected number of new cases E becomes minimum for* $(\alpha, q) = (\alpha^*, 1)$ *in the region* $\{(\alpha, q) \in (0, 1) \times (0, 1) \mid \alpha \le \alpha_c \in (0, 1)$ *and* $q > q_c \in (0, 1)\}$.

Lastly, the case of $(\alpha, q) = (\alpha^*, q^*)$ could be valid for minimizing E only when $\alpha > \alpha_c \in (0, 1)$ and $q > q_c \in (0, 1)$. Now suppose that it could be valid. We have q^* for $\alpha = \alpha^*$ satisfying the following from $\psi_q(\alpha^*, q^*) = 0$ by (B.3) in the proof of Theorem 4.1:

$$-3\alpha^{*3} + \left(3 + \frac{2}{q^*}\right)\alpha^{*2} + \frac{2A}{q^*}\alpha^* - \frac{2}{\sigma_s N q^{*2}} = 0, \tag{D.3}$$

while α^* for $q = q^*$ satisfies the following from (5.2) in Theorem 5.1:

$$-4\alpha^{*3} + \left(3 + \frac{3}{q^*}\right)\alpha^{*2} + \frac{2A}{q^*}\alpha^* - \frac{2}{\sigma_s N q^{*2}} = 0,$$

that is,

$$-3\alpha^{*3} + \left(3 + \frac{2}{q^*}\right)\alpha^{*2} + \frac{2A}{q^*}\alpha^* - \frac{2}{\sigma_s N q^{*2}} = \alpha^{*3} - \frac{\alpha^{*2}}{q^*}. \tag{D.4}$$

From these Eqs. (D.3) and (D.4), we can immediately get the equation that $\alpha^{*3} - \alpha^{*2}/q^* = 0$, which results in $\alpha^* q^* = 1$. This is inconsistent for $\alpha^* \in (0, 1)$ and $q^* \in (0, 1)$. This means that there does not exist mathematically reasonable (α^*, q^*) such that $\alpha^* \in (0, 1)$ and $q^* \in (0, 1)$ about E. Finally we can conclude the following lemma:

Lemma D.3. *There is no definite point* (α, q) *to minimize* E *in the region* $\{(\alpha, q) \in (0, 1) \times (0, 1) \mid \alpha > \alpha_c \in (0, 1)$ *and* $q > q_c \in (0, 1)\}$.

This lemma indicates that the expected number of new cases E cannot be minimum when $\alpha = \alpha^* \in (0, 1)$ and $q = q^* \in (0, 1)$, and further implies that it becomes minimum only when $\alpha = 1$ or $q = 1$. Consequently, we can derive Theorem 6.1.